Polymer Chemistry

Sustainable Synthesis of CO2–derived Polycarbonates from D Xylose

Journal:	*Polymer Chemistry*
Manuscript ID	PY-COM-06-2021-000784.R1
Article Type:	Communication
Date Submitted by the Author:	02-Sep-2021
Complete List of Authors:	Tran, David; Texas A&M University, Chemistry Rashad, Ahmed; Texas A&M University, Chemistry Darensbourg, Donald; Texas A&M University Wooley, Karen; Texas A&M University, Chemistry

COMMUNICATION

Sustainable Synthesis of CO_2–derived Polycarbonates from D-Xylose

Received 00th January 20xx,
Accepted 00th January 20xx

DOI: 10.1039/x0xx00000x

David K. Tran,[a] Ahmed Z. Rashad,[a] Donald J. Darensbourg,*[a] and Karen L. Wooley *[a,b,c]

Synthetic transformation of D-xylose into a four-membered cyclic ether allows for reactions with carbon dioxide (CO_2) leading to linear polycarbonates by either a one-step ring-opening copolymerisation (ROCOP) directly, or by sequential isolation of a preformed six-membered cyclic carbonate followed by ring-opening polymerisation (ROP).

Introduction

Over the past century, plastics have become an integral part of daily life, being utilized in numerous applications, including healthcare, packaging, transportation, and electronics, among others. Despite their overall importance, many polymeric materials are synthesized from petroleum-based chemicals and can persist for excessively long periods of time, providing stresses on the environment.[1] There is, therefore, a growing shift toward the use of sustainably-sourced feedstocks for the production of degradable polymers, bioplastics. However, there is also an increasing realization that natural building blocks may not be able to entirely replace petrochemicals, due to lack of both sufficient quantity and economic viability. We argue, instead, that a critical need is actually the development of synthetic routes that incorporate complementary feedstocks, those which come from multiple natural, petrochemical and even humanmade sources. By such processes, a greater balance may be achieved between the quantity of biomass that can be harvested without adverse competition *vs*. food needs for the worldwide growing population, and the amounts of fossil-based feedstocks that can be extracted as they are on the decline.[2] In alignment with these aims, a particular emphasis has emerged, recently, involving the development of synthetic methodologies by which to harness combinations of natural products and carbon dioxide for the production of degradable bioplastics.

Carbohydrates, polysaccharides and other polymers comprised of carbohydrate repeat units are ubiquitous natural products that provide models for synthetic materials development. In the plant and animal kingdoms of Nature, these sugar-based macromolecules play vital roles in living systems, from energy storage (*e.g.*, starch), to molecular recognition and cell signalling (*e.g.*, glycoproteins), to cellular data storage machinery (*e.g.*, DNA, RNA), to structural purposes (*e.g.*, cellulose).[3] As renewable biomass, polysaccharides also produce valuable commodities used in manufacturing processes.[4] They contain classes of molecules and macromolecules with structurally rich compositions and structures, providing diverse feedstocks for synthetic polymer development. An increasing interest is focused upon developing synthetic polymers that mimic these naturally-

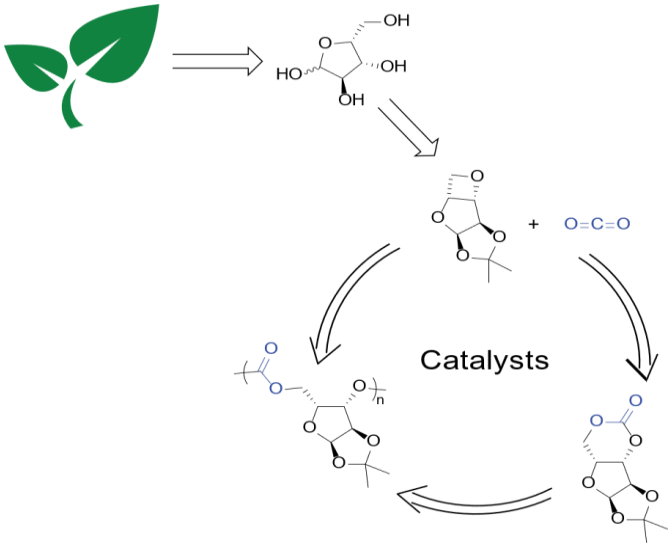

Figure 1. Overall synthetic approach to produce linear polycarbonate derived from naturally sourced D-xylose.

[a] Department of Chemistry, Texas A&M University, College Station, Texas 77843, United States. Email: djdarens@chem.tamu.edu, wooley@chem.tamu.edu
[b] Department of Chemical Engineering, Texas A&M University, College Station, Texas 77843, United States
[c] Department of Materials Science & Engineering, Texas A&M University, College Station, Texas 77843, United States

† Electronic Supplementary Information (ESI) available. See DOI: 10.1039/x0xx00000x

occurring macromolecules, while expanding the chemical scope to incorporate selectively-degradable linkages and probe, fundamentally, composition-structure-property relationships. As a result, carbohydrate-based monomers have been developed, used, and studied to afford polyesters,[5] polyurethanes,[6] polyamides,[7] polyphosphoesters,[8, 9] and polycarbonates,[10] promoting sustainability, biocompatibility, multifunctionality, and degradability.

Among the different classes of sugar-derived polymers, we have focused upon the use of D-glucose for the construction of compositionally- and regiochemically-diverse polycarbonates,[11-16] due to the potential to achieve a range of thermal and mechanical properties, analogous to both cellulose and polycarbonate engineering plastics, while also providing routes for hydrolytic degradation to release the glucose sugar and carbon dioxide. These poly(D-glucose carbonate)s have been synthesized by transforming D-glucose to a five- or six-membered cyclic carbonate followed by ROP, or through formation of a diol followed by polycondensation. However, both of these methods have involved the use of phosgene derivatives to establish the carbonate functionalities, which although highly effective, is not ideal for safety and environmental concerns. Hence, there is a need to shift this synthetic methodology into one that is not dependent on phosgene. Elimination of phosgene dependence has been achieved by the Buchard[17-19] and Gnanou[20] groups. These two groups have used CO_2 as a carbonylation reagent by either coupling CO_2 with diols to afford five- to eight-membered cyclic carbonates,[21] excellent materials for ROP, or by incorporating CO_2 directly as a reagent with dihalides and diols for polycondensation.[20, 22]

Ring-opening copolymerisation (ROCOP) is a versatile technique that relies on the combination of two or more comonomers, at least one of which is cyclic. This polymerisation

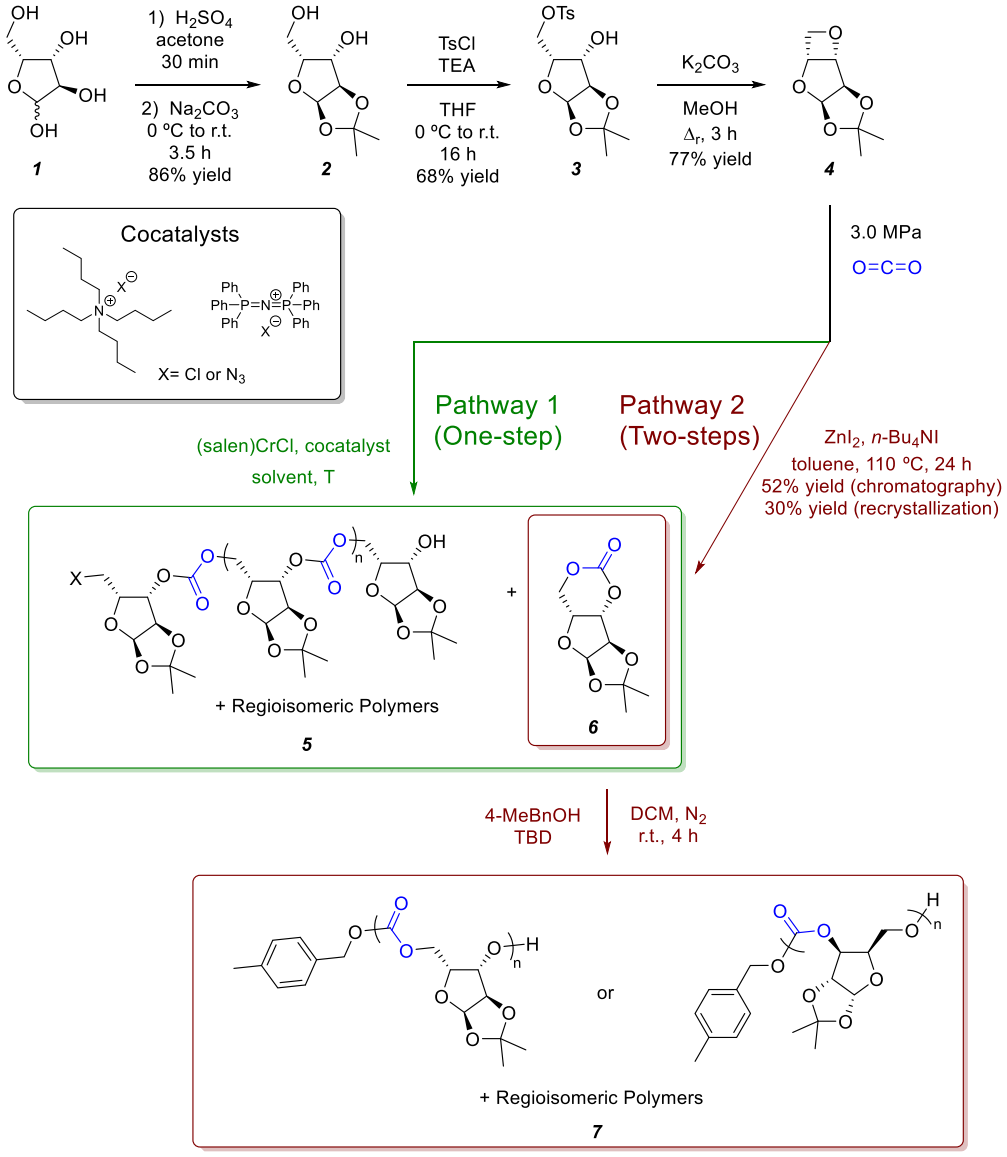

Scheme 1. Synthesis of 3,5-anhydro-1,2-*O*-isoproylidene-α-D-xylofuranose, where pathway 1 is the synthetic route for producing poly(1,2-isoproylidene-α-D-xylofuranose carbonate) through ring-opening copolymerisation, and pathway 2 is the synthetic route for producing first 1,2-isoproylidene-α-D-xylofuranose carbonate, followed by poly(1,2-*O*-isoproylidene-α-D-xylofuranose carbonate) through organocatalysed ring-opening polymerisation.

methodology generates highly functional copolymers with narrow dispersities, diverse linkages, and versatile end group compositions.[23-28] Amongst the types of ROCOP, we have had a long-standing interest in copolymerisations involving carbon dioxide (CO_2) as a comonomer,[29-40] due to the ability to achieve carbon fixation and also create materials that are carbon neutral upon degradation. Typically, this copolymerisation uses a strained cyclic ether, such as an oxirane[41-46] or oxetane,[47-51] with CO_2 to afford polycarbonates that, theoretically, can contain up to 50 mol% of CO_2. Although these CO_2-derived polycarbonates are of great interest, comonomers obtained from sustainable origins have received limited attention.[32] Moreover, relative to oxiranes, oxetanes have been under-utilized, likely due to their laborious syntheses which translate to reduced commercial accessibilities.[29]

Of the various ROCOP combinations, we were inspired to investigate the catalytic coupling reaction of CO_2 with an oxetane synthesized from a naturally-derived carbohydrate, D-xylose. Given previous work on the copolymerisation of CO_2 with oxetanes derived from petrochemical sources,[47-51] we were keen to undertake this synthetic challenge. Herein, we describe a dual synthetic approach that produces polycarbonates either through direct transition metal-mediated ROCOP of an oxetane derived from D-xylose with CO_2 or through a two-step process, first transforming the oxetane into a six-membered cyclic carbonate followed by organobase-catalysed ROP (**Fig. 1**).

Results and Discussion

To incorporate D-xylose into polycarbonates, each synthetic approach relied upon the production of α-D-xylofuranose having the four-membered cyclic ether installed through the 3- and 5-positions, and the 1- and 2- positions protected to avoid their participation during ROCOP or ROP (**Fig. 1** and **Scheme 1**). Protection was achieved through selective ketalization of D-xylose (***1***) using acetone and sulphuric acid, which initially generated the five- and six-membered cyclic ketals at the 1- and 2- and the 3- and 5- positions of ***1***, respectively. Treatment with Na_2CO_3 promoted selective cleavage of the six-membered cyclic ketal allowing for isolation of 1,2-*O*-isopropylidene-α-D-xylofuranose (***2***). The oxetane was then generated through a two-step process. Monotosylation of the primary alcohol was first performed using ***2***, triethylamine, and tosyl chloride in THF to afford 1,2-*O*-isopropylidene-5-*O*-tosyl-α-D-xylofuranose (***3***). Intramolecular cyclization was then performed using the hydroxyl group at the 3-position of ***3*** in the presence of K_2CO_3, producing 3,5-anhydro-1,2-*O*-isopropylidene-α-D-xylofuranose (***4***) in 77% yield after distillation over CaH_2.

D-Xylose-derived polycarbonates (***5***) were produced directly by an alternating ROCOP of CO_2 with ***4*** in the presence of metal catalyst (salen)CrCl and cocatalyst bis(triphenylphosphine)iminium chloride (PPNCl) (**Scheme 1**, *Pathway 1*). Initial studies were performed in in-house stainless steel autoclave reactors using conditions from our previous investigations, *i.e.*, 110 °C, 3.0 MPa CO_2, in toluene.[48-52] A [monomer]:[catalyst] ratio of 250:1 resulted in only 37% conversion of ***4***, and the reaction slightly favoured cyclic carbonate (***6***) formation over the copolymer (***5***). Therefore, the [monomer]:[catalyst] ratios were decreased until higher oxetane conversions and copolymer selectivities were acquired (entries 1-3 in **Table 1**). At a ratio of 75:1, a copolymer selectivity of ~67% was observed, along with an increase in oxetane conversion.

Using the 75:1 [monomer]:[catalyst] ratio, different cocatalysts were then screened to further increase the selectivity towards the copolymer (***5***) over the cyclic carbonate (***6***) (entries 3-5 in **Table 1**). There was a significant effect on the resulting product ratio based on the identity of the cocatalyst cation and its counter anion. PPNCl performed better as a cocatalyst compared to tetrabutyl ammonium chloride (*n*-Bu_4NCl), due to higher selectivity for the copolymer (*c.f.* entries 3 and 5 in **Table 1**). This effect is attributed to the copolymerisation favouring cocatalysts that possess a noninteracting cation like PPN^+, which has a positive charge delocalized over a large molecular volume.[31] Using the PPNX cocatalyst system, azide was then selected as the counter anion because azides are good nucleophiles but poor leaving groups. Although these properties can be advantageous during

Table 1. Alternating CO_2/Xylose Oxetane Copolymerisation Catalysed by (salen)CrCl/ Onium Salt Catalytic System[a]

Entry	Catalyst	Cocatalyst	Cat.:Cocat.:Oxetane	Solvent	T (°C)	% conv.[b]	Copolymer[c]	Cyclic Carbonate[c]	$M_{n,SEC}$ (kDa)[d]	$Đ^d$
1	(salen)CrCl	PPNCl	1:2:250	toluene	110	37	43%	57%	8.9	1.21
2	(salen)CrCl	PPNCl	1:2:150	toluene	110	37	49%	51%	7.1	1.14
3	(salen)CrCl	PPNCl	1:2:75	toluene	110	60	67%	33%	6.9	1.07
4	(salen)CrCl	$PPNN_3$	1:2:75	toluene	110	43	46%	54%	7.8	1.26
5	(salen)CrCl	*n*-Bu_4NCl	1:2:75	toluene	110	25	27%	73%	6.9	1.14
6	(salen)CrCl	PPNCl	1:2:75	xylenes	110	47	52%	48%	5.9	1.13
7	(salen)CrCl	PPNCl	1:2:75	xylenes	120	47	51%	49%	5.8	1.13
8	(salen)CrCl	PPNCl	1:2:75	xylenes	130	42	51%	49%	6.4	1.12
9	(salen)CrCl	PPNCl	1:2:75	xylenes	140	61	80%	20%	7.4	1.12

[a]Reactions were performed in a 10 mL autoclave; [(salen)CrCl]/[cocatalyst] = ½, molar ratios for 72 h with 3.0 MPa CO_2. Degrees of alternation were >99% based for all samples based on ^{1}H NMR spectroscopy. [b]Oxetane conversions were determined by ^{1}H NMR spectroscopy of the crude mixture. [c]Molar ratios of the copolymer *vs.* cyclic carbonate, were determined by ^{1}H NMR spectroscopy of the crude mixture. [d]Molar masses of polymers isolated from precipitation in methanol were determined by size exclusion chromatography in THF, calibrated with polystyrene standards.

COMMUNICATION

Figure 2. ^{1}H NMR spectra of poly(1,2-*O*-isopropylidene-α-D-xylofuranose carbonate) ***5*** from ROCOP (red trace), 3,5-anhydro-1,2-*O*-isopropylidene-α-D-xylofuranose (***4***, green trace), 1,2-*O*-isopropylidene-α-D-xylofuranose carbonate (***6***, blue trace), and poly(1,2-*O*-isopropylidene-α-D-xylofuranose carbonate) ***7*** from organocatalysed ROP (purple trace), where the chemical shift of the anomeric position of each compound is located in the highlighted region.

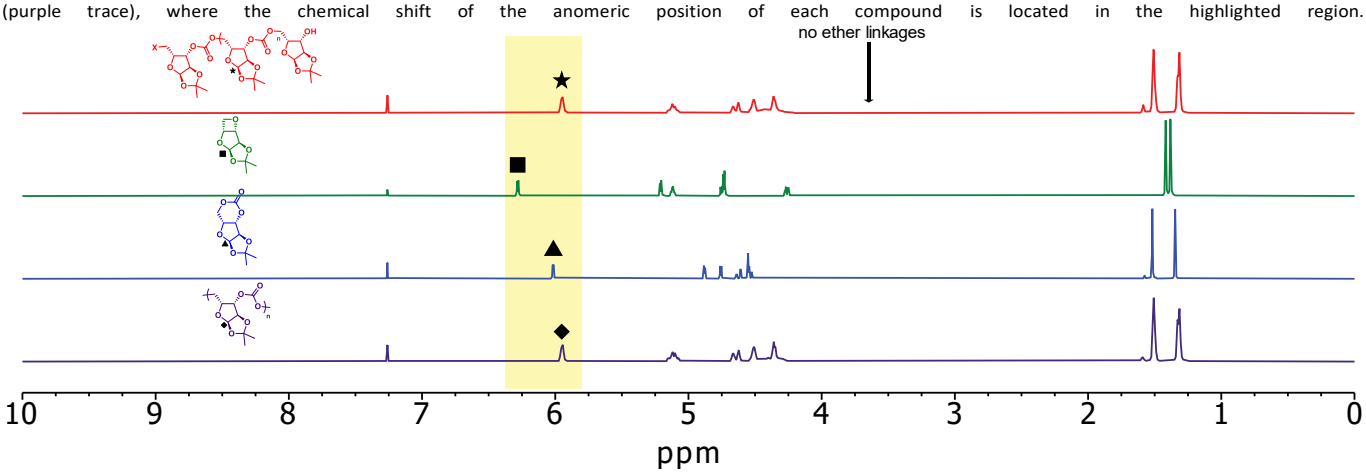

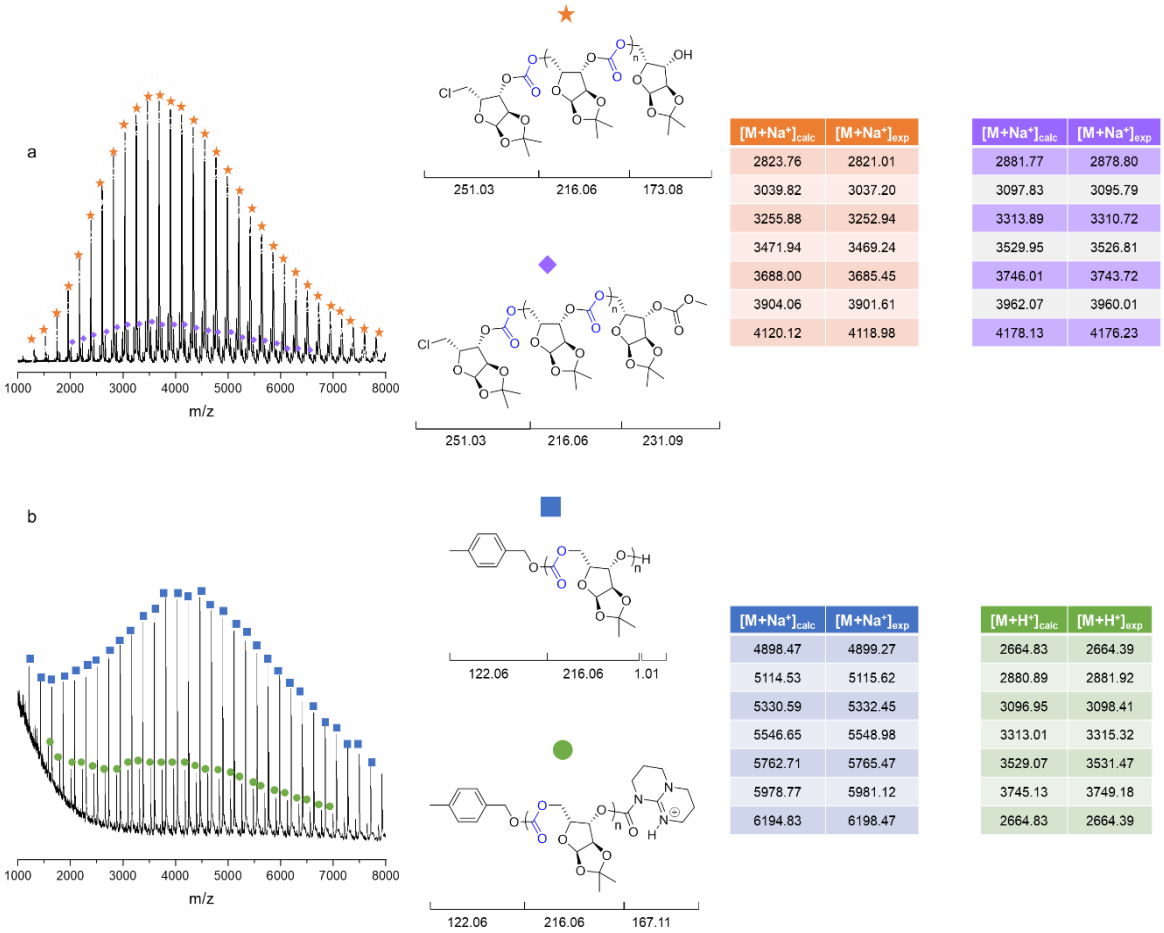

$[M+Na^+]_{calc}$	$[M+Na^+]_{exp}$
2823.76	2821.01
3039.82	3037.20
3255.88	3252.94
3471.94	3469.24
3688.00	3685.45
3904.06	3901.61
4120.12	4118.98

$[M+Na^+]_{calc}$	$[M+Na^+]_{exp}$
2881.77	2878.80
3097.83	3095.79
3313.89	3310.72
3529.95	3526.81
3746.01	3743.72
3962.07	3960.01
4178.13	4176.23

$[M+Na^+]_{calc}$	$[M+Na^+]_{exp}$
4898.47	4899.27
5114.53	5115.62
5330.59	5332.45
5546.65	5548.98
5762.71	5765.47
5978.77	5981.12
6194.83	6198.47

$[M+H^+]_{calc}$	$[M+H^+]_{exp}$
2664.83	2664.39
2880.89	2881.92
3096.95	3098.41
3313.01	3315.32
3529.07	3531.47
3745.13	3749.18
2664.83	2664.39

Figure 3. MALDI-ToF spectra of (a) copolymer produced from ROCOP of CO_2 and xylose oxetane. (b) polymer produced from TBD-catalysed ROP of 1,2-*O*-isopropylidene-α-D-xylofuranose carbonate.

copolymerisation to minimize cyclic carbonate by-product, the selectivity and conversion decreased using $PPNN_3$, contrary to previous studies.[47, 49]

In an effort to increase copolymer selectivity while maintaining moderate conversion, the copolymerisation was then investigated in the presence of (salen)CrCl and PPNCl at increased temperatures. The solvent was replaced with xylenes (b.p. ~140 °C), and experiments were conducted from 110 – 140 °C (entries 6-9 in **Table 1**). At temperatures of 110 – 130 °C, copolymer selectivity remained unchanged. At a temperature of 140 °C, however, there was a significant improvement in the selectivity (~80%). This improvement can result from shifting the reaction towards formation of the thermodynamic product ***5*** through ring-opening reactions of the six-membered cyclic carbonate intermediate ***6***.

Figure 2 highlights the possible products, isolated and purified, from the coupling of ***4*** with CO_2. For each ROCOP reaction, the six-membered cyclic carbonate, 1,2-*O*-isopropylidene-α-D-xylofuranose carbonate (***6***) was observed. In addition, there were no ether linkages formed during the copolymerisations, as indicated by ^{1}H NMR spectroscopy. The relative quantities of copolymer ***5*** along with any unreacted oxetane ***4***, cyclic carbonate ***6***, carbonate linkages, and/or ether linkages were determined by integrating the protons resonating at 6.20 ppm, 6.02 ppm, 5.90 ppm, and 3.60 ppm, respectively, in the ^{1}H NMR spectra of crude mixtures. In addition to the absence of ether proton signals in the ^{1}H NMR spectra, the degrees of alternation of ***5*** were further supported by matrix-assisted laser desorption ionization time-of-flight (MALDI-ToF). Analysis of a low molar mass copolymer sample revealed two series of peaks, where the major species indicated chlorine and O-H end groups while the minor species indicated a chlorine and methyl carbonate end group (**Fig. 3a**). Each series of peaks showed a separation of 216 m/z, which corresponds to the repeating unit of 1,2-*O*-isopropylidene-α-D-xylofuranose and CO_2. ^{13}C NMR spectroscopy indicated that ***5*** was regioirregular, based on the carbonyl region. Three resonances were observed at 154.57, 153.92, and 153.38 ppm consistent with tail-to-tail, head-to-tail, and head-to-head linkages, respectively (**Fig. S10†**). It is suspected that this regioirregularity arose from the growing anion chain of the copolymer participating in the ring-opening of intermediate ***6*** during the copolymerisation.

To further understand mechanistic aspects of the coupling of CO_2 with ***4***, reaction kinetics were studied at 110 °C. Unfortunately, *in-situ* infrared spectroscopy could not be used to monitor the copolymerisation, therefore, several reactions were conducted under the same conditions and then quenched and analysed at different time points. The ROCOP proceeded slowly (**Fig. 4a** and **Table S1†**), likely due to the steric bulkiness of ***4*** inhibiting the four-membered cyclic ether from binding to Cr. Relatively slow kinetics were similarly observed for other bulky oxirane substrates, such as naphthalene oxide and indene oxide, for which low molar masses were obtained using (salen)CrCl.[53, 54] These kinetic studies also revealed that cyclic carbonate formation (***6***) was preferred over the copolymer (***5***) during the early stages of copolymerisation (**Fig. 4b**), which can

Figure 4. (a) % conversion *versus* time of copolymerisation of xylose oxetane with CO_2 (b) % selectivity of the cyclic carbonate and copolymer as a function of time during the copolymerisation.

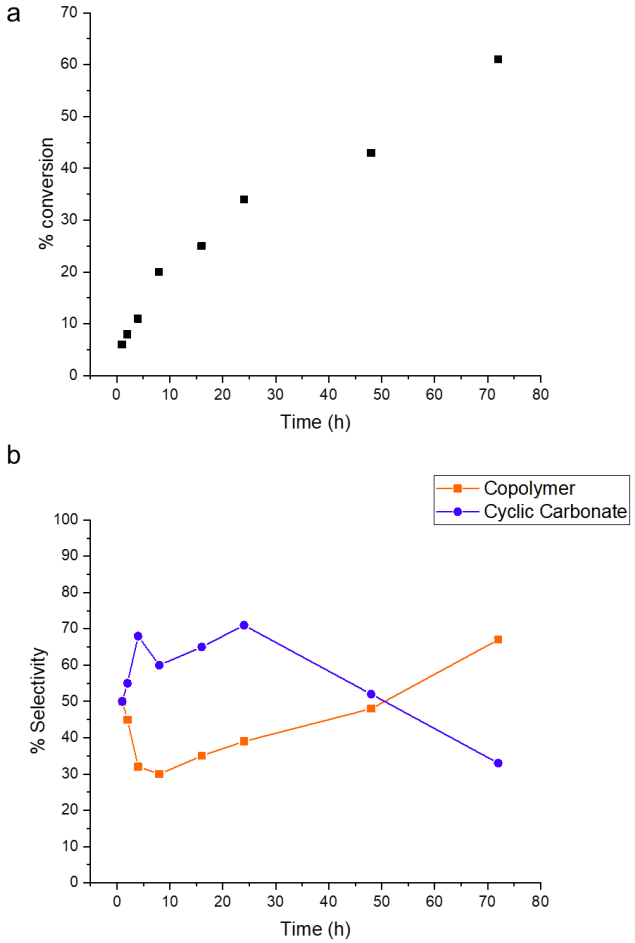

be attributed to a back-biting reaction of the growing polymer chain end. However, after 24 hours, there was a progressive decrease in cyclic carbonate concentration with a concomitant increase in copolymer formation. Unlike typical five-membered cyclic carbonates formed from reactions of CO_2 with epoxides, this six-membered cyclic carbonate (***6***) is capable of undergoing ROP, due to both its ring size and its tricyclic structure. These findings strongly suggest that ***4*** behaves similarly to sterically-hindered oxetanes, such as 3-benzyloxymethyl-3-methyloxetane, showing a similar trend where cyclic carbonate (kinetic product) is preferred at the initial stage of ROCOP, but the linear polycarbonate (thermodynamic product) is favoured, ultimately.[51]

The slight preference for the cyclic carbonate at the initial stages of the copolymerisation inspired us to investigate an alternative pathway to polycarbonate formation (**Scheme 1**, *Pathway 2*), one in which the six-membered cyclic carbonate became a synthetic target for subsequent organobase-catalysed ROP. Therefore, our focus shifted to determining conditions for reaction of ***4*** with CO_2 that led predominantly to cyclic carbonate formation. Since the CO_2 coupling reaction was

COMMUNICATION

Table 2. CO_2 Coupling with Xylose Oxetane Using ZnI_2[a]

Entry	Catalyst	Cocatalyst	Catalyst:Cocatalyst:Oxetane	% conv.[b]	Cyclic Carbonate[c]	Oligomer[c]
1	(salen)CrCl	*n*-Bu_4NCl	1:3:10	88	52%	48%
2	ZnI_2	PPNI	1:3:10	92	54%	46%
3	ZnI_2	*n*-Bu_4NI	1:3:75	13	>99%	0%
4	ZnI_2	*n*-Bu_4NI	1:3:50	21	>99%	0%
5	ZnI_2	*n*-Bu_4NI	1:3:25	33	>99%	0%
6	ZnI_2	*n*-Bu_4NI	1:3:10	44	>99%	0%

[a] Reactions were performed in toluene; [catalyst]/[cocatalyst] = 1:3 molar ratios in a 10 mL autoclave for 24 h. [b]Oxetane conversions were determined by ^1H NMR spectroscopy of the crude mixture. [c]Molar ratios of the oligomer *vs.* cyclic carbonate, were determined by ^1H NMR spectroscopy of the crude mixture.

performed using (salen)CrCl and PPNCl, which resulted in a mixture of ***5*** and ***6***, the next step was to substitute the cocatalyst for one that interacts with the growing polymer chain end to promote formation of the cyclic product. *n*-Bu_4NCl was selected, and it was observed that cyclic carbonate was favoured (entry 1 in **Table 2**). Unfortunately, under these conditions ring-opening reactions of the six-membered cyclic carbonate may also be promoted, as observed by the formation of a nearly equal molar equivalence of ring-opened oligomers.

Therefore, both the metal catalyst and cocatalyst were screened (entries 1-3 in **Table 2**) to facilitate cycloaddition *via* opening of the oxetane with CO_2 insertion, while avoiding cyclic carbonate ring-opening reactions. Zinc halide catalysts have been shown to play essential roles for CO_2 coupling reactions with oxiranes, producing five-membered cyclic carbonates.[30, 55] From past investigations, iodide was identified as a superior leaving group among a series of anions, *i.e.* Cl^-, Br^-, and N_3^-. In addition, iodide is also a poorer nucleophile, which can inhibit ring-opening reactions.[56, 57] Therefore, the metal catalyst was selected to be ZnI_2. Furthermore, cocatalysts PPNI and *n*-Bu_4NI were studied. Reactions were performed using 3.0 MPa CO_2 with ***4***, ZnI_2, and cocatalyst, PPNI or *n*-Bu_4NI, in toluene for 24 hours to determine which cocatalyst favoured cyclic carbonate over oligomer. ^1H NMR spectroscopy initially indicated that PPNI was a better cocatalyst compared to *n*-Bu_4NI, due to higher oxetane conversion (~90%) (entry 2 in **Table 2**). However, there was only a 54% selectivity for the six-membered cyclic carbonate production. Reactions involving *n*-Bu_4NI showed that regardless of catalyst to oxetane loading, there was a predominate preference for the cyclic carbonate product, despite low conversions (entries 3-6 in **Table 2**).

The CO_2 coupling reaction with ***4*** was scaled-up using ZnI_2 and *n*-Bu_4NI as the catalyst and cocatalyst, respectively, to allow for isolation and characterisation of this alternative monomer ***6***. FT-IR analysis showed the appearance of a carbonyl peak at 1732 cm^{-1}, which indicated the formation of the cyclic carbonate (**Fig. S13†**). ^1H and ^{13}C NMR data were in agreement with the expected chemical structure (**Fig. S5†** and **S11†**). Moreover, a single crystal was grown and was verified by x-ray crystallography to confirm the absolute structure (**Fig. S15†**).

By this secondary pathway, ***6*** then underwent ROP to afford well-defined polycarbonates. The organobase-catalysed ROP of ***6*** was performed with 1,5,7-triazabicyclo-[4.4.0]dec-5-ene (TBD), which had previously shown excellent control in the ROP of cyclic carbonate monomers.[15, 19, 58-62] The polymerisation of ***6*** initiated by 4-methylbenzyl alcohol in the presence of TBD at room temperature reached over 60% conversion in 4 hours, producing poly(1,2-*O*-isopropylidene-α-D-xylofuranose carbonate) ***7*** with a molar mass of 10 kDa and a dispersity (*Đ*) < 1.2. MALDI-ToF analysis revealed no evidence of transesterification and confirmed the expected 4-methylbenzyl and O-H end groups for a linear polymer series with each peak having a difference of 216 m/z, which corresponds to the molar mass of the repeating unit (**Fig. 3b**). Similar to polycarbonates formed from ROCOP, ^{13}C NMR indicated the characteristic resonance for a carbonate linkage with three observed signals at 154.57, 153.90, and 153.39 ppm, consistent with tail-to-tail, head-to-tail, and head-to-head linkages, respectively (**Fig. S12†**). This regioirregularity arises from the cleavage of either the CX-O3 or the CX-O5 bond of the tetrahedral intermediate from the asymmetric carbonate, generating a free secondary or primary propagating alcohol chain end, respectively. This regioirregularity has also been observed for other furanose- and pyranose-based polycarbonates, the repeat unit chemical structures of which correspond to those of ***7***.[13, 17, 63]

Notably, given the same backbone compositions and relatively benign chain end functional group contributions to the physicochemical properties, the polycarbonates of xylose and CO_2 obtained from both the ROCOP and cycloaddition+ROP pathways were determined to have similar thermal characteristics. Glass transition temperatures were determined to be at 121 °C and 125 °C (**Figure S16†**) for ROCOP and ROP, respectively, with no apparent crystallization or melting transitions. Each also underwent complete thermal decomposition with 100% mass loss over a relatively low and narrow temperature range of 180-260 °C and 200-280 °C (**Figure**

S17†) for ROCOP and ROP, respectively. Although the low thermal stability may be a disadvantage in applications that would require high temperatures, it may also provide opportunities for use as a thermally ablative material.

Conclusions

We have demonstrated a dual-pathway strategy by which to incorporate renewable biomass in the form of naturally-derived carbohydrate building blocks to achieve polycarbonate production, from an oxetane derived from D-xylose with the consumption of CO_2. This four-membered cyclic ether substrate expands the current library of oxetanes that have been combined with CO_2 to those originating from natural feedstocks. The first approach involves ring-opening copolymerisation of the oxetane with CO_2 through the use of the (salen)CrCl and PPNCl system. The second approach focused on transforming the oxetane into a six-membered cyclic carbonate using ZnI_2/*n*-Bu_4NI, followed by organobase-catalysed ROP to afford the polycarbonate. Each approach yielded similar polycarbonates, however, with important differences in the chain end compositions and degrees of control over molar masses. Overall, their physicochemical and thermal characteristics agreed well, as determined by FT-IR, ^1H and ^{13}C NMR spectroscopies and by differential scanning calorimetry and thermogravimetric analysis. Their chain end compositional differences were confirmed by MALDI-ToF mass spectrometry. The ROCOP approach has the advantage of involving a single step, whereas the two-step ROP pathway allowed for the production of polycarbonates having higher degrees of polymerisation and within shorter periods of time. Overall, the two synthetic approaches highlight the potential of combining CO_2 as an abundant C1 feedstock with monomers derived from renewable sources, through a relatively economically-viable, safe and sustainable methodology, to afford polycarbonates having a diversity of chain end and backbone structures and compositions. Future work will involve the exploration of different catalyst systems to improve the selectivity for copolymer over cyclic carbonate during ROCOP. Additionally, investigation of methodologies to convert this sugar-derived oxetane to its six-membered cyclic carbonate counterpart using metal-free conditions are of interest. For both systems, studies of the regiochemical details are also being pursued.

Conflicts of interest

The authors declare no competing financial interest.

Acknowledgements

We gratefully acknowledge financial support from the National Science Foundation under grant numbers CHE-2003771 and DMR-1905818, and the Welch Foundation through the W. T. Doherty-Welch Chair in Chemistry under grant number A-0001. We thank Dr. Nattamai Bhuvanesh (Department of Chemistry, Texas A&M University) for assistance with single-crystal and x-ray powder diffractometry and Dr. Yohannes Rezenom (Department of Chemistry, Texas A&M University) for assistance with mass spectrometry.

Notes and references

1. B. C. Gibb, *Nat. Chem.*, 2019, **11**, 394-395.
2. G. W. Coates and Y. D. Y. L. Getzler, *Nat. Rev. Mater.*, 2020, **5**, 501-516.
3. R. Stern and M. J. Jedrzejas, *Chem. Rev.*, 2008, **108**, 5061-5085.
4. A. J. Ragauskas, C. K. Williams, B. H. Davison, G. Britovsek, J. Cairney, C. A. Eckert, W. J. Frederick, J. P. Hallett, D. J. Leak, C. L. Liotta, J. R. Mielenz, R. Murphy, R. Templer and T. Tschaplinski, *Science*, 2006, **311**, 484-489.
5. W. C. Shearouse, L. M. Lillie, T. M. Reineke and W. B. Tolman, *ACS Macro Lett.*, 2015, **4**, 284-288.
6. Z. Mou, S. Feng and E. Y. X. Chen, *Polym. Chem.*, 2016, **7**, 1593-1602.
7. E. L. Dane and M. W. Grinstaff, *J. Am. Chem. Soc.*, 2012, **134**, 16255-16264.
8. Y.-Y. Tsao, T. H. Smith and K. L. Wooley, *ACS Macro Lett.*, 2018, **7**, 153-158.
9. Y.-Y. Tsao and K. L. Wooley, *J. Am. Chem. Soc.*, 2017, **139**, 5467-5473.
10. L. Su, S. Khan, J. Fan, Y.-N. Lin, H. Wang, T. P. Gustafson, F. Zhang and K. L. Wooley, *Polym. Chem.*, 2017, **8**, 1699-1707.
11. A. T. Lonnecker, Y. H. Lim, S. E. Felder, C. J. Besset and K. L. Wooley, *Macromolecules*, 2016, **49**, 7857-7867.
12. A. T. Lonnecker, Y. H. Lim and K. L. Wooley, *ACS Macro Lett.*, 2017, **6**, 748-753.
13. K. Mikami, A. T. Lonnecker, T. P. Gustafson, N. F. Zinnel, P.-J. Pai, D. H. Russell and K. L. Wooley, *J. Am. Chem. Soc.*, 2013, **135**, 6826-6829.
14. S. E. Felder, M. J. Redding, A. Noel, S. M. Grayson and K. L. Wooley, *Macromolecules*, 2018, **51**, 1787-1797.
15. Y. Song, X. Yang, Y. Shen, M. Dong, Y.-N. Lin, M. B. Hall and K. L. Wooley, *J. Am. Chem. Soc.*, 2020, **142**, 16974-16981.
16. Y. Song, X. Ji, M. Dong, R. Li, Y.-N. Lin, H. Wang and K. L. Wooley, *J. Am. Chem. Soc.*, 2018, **140**, 16053-16057.
17. G. L. Gregory, E. M. Hierons, G. Kociok-Köhn, R. I. Sharma and A. Buchard, *Polym. Chem.*, 2017, **8**, 1714-1721.
18. G. L. Gregory, L. M. Jenisch, B. Charles, G. Kociok-Köhn and A. Buchard, *Macromolecules*, 2016, **49**, 7165-7169.
19. G. L. Gregory, G. Kociok-Köhn and A. Buchard, *Polym. Chem.*, 2017, **8**, 2093-2104.
20. D. Pati, Z. Chen, X. Feng, N. Hadjichristidis and Y. Gnanou, *Polym. Chem.*, 2017, **8**, 2640-2646.
21. T. M. McGuire, E. M. López-Vidal, G. L. Gregory and A. Buchard, *J. CO_2 Util.*, 2018, **27**, 283-288.
22. Z. Chen, N. Hadjichristidis, X. Feng and Y. Gnanou, *Polym. Chem.*, 2016, **7**, 4944-4952.
23. B. A. Abel, C. A. L. Lidston and G. W. Coates, *J. Am. Chem. Soc.*, 2019, **141**, 12760-12769.
24. C. A. L. Lidston, B. A. Abel and G. W. Coates, *J. Am. Chem. Soc.*, 2020, **142**, 20161-20169.

25. S. Wu, M. Luo, D. J. Darensbourg and X. Zuo, *Macromolecules*, 2019, **52**, 8596-8603.
26. M. Jurrat, B. J. Pointer-Gleadhill, L. T. Ball, A. Chapman and L. Adriaenssens, *J. Am. Chem. Soc.*, 2020, **142**, 8136-8141.
27. T. T. D. Chen, L. P. Carrodeguas, G. S. Sulley, G. L. Gregory and C. K. Williams, *Angew. Chem. Int. Ed.*, 2020, **59**, 23450-23455.
28. L. P. Carrodeguas, T. T. D. Chen, G. L. Gregory, G. S. Sulley and C. K. Williams, *Green Chem.*, 2020, **22**, 8298-8307.
29. G. A. Bhat, M. Luo and D. J. Darensbourg, *Green Chem.*, 2020, **22**, 7707-7724.
30. D. J. Darensbourg, S. J. Lewis, J. L. Rodgers and J. C. Yarbrough, *Inorg. Chem.*, 2003, **42**, 581-589.
31. D. J. Darensbourg and R. M. Mackiewicz, *J. Am. Chem. Soc.*, 2005, **127**, 14026-14038.
32. S. J. Poland and D. J. Darensbourg, *Green Chem.*, 2017, **19**, 4990-5011.
33. D. J. Darensbourg, J. R. Wildeson, S. J. Lewis and J. C. Yarbrough, *J. Am. Chem. Soc.*, 2002, **124**, 7075-7083.
34. D. J. Darensbourg, B. J. Frost and D. L. Larkins, *Inorg. Chem.*, 2001, **40**, 1993-1999.
35. D. J. Darensbourg, P. Rainey and J. Yarbrough, *Inorg. Chem.*, 2001, **40**, 986-993.
36. C. Koning, J. Wildeson, R. Parton, B. Plum, P. Steeman and D. J. Darensbourg, *Polymer*, 2001, **42**, 3995-4004.
37. D. J. Darensbourg and M. S. Zimmer, *Macromolecules*, 1999, **32**, 2137-2140.
38. D. J. Darensbourg, S. A. Niezgoda, J. D. Draper and J. H. Reibenspies, *J. Am. Chem. Soc.*, 1998, **120**, 4690-4698.
39. D. J. Darensbourg, E. L. Maynard, M. W. Holtcamp, K. K. Klausmeyer and J. H. Reibenspies, *Inorg. Chem.*, 1996, **35**, 2682-2684.
40. D. J. Darensbourg, M. W. Holtcamp, B. Khandelwal, K. K. Klausmeyer and J. H. Reibenspies, *J. Am. Chem. Soc.*, 1995, **117**, 538-539.
41. M. Jia, N. Hadjichristidis, Y. Gnanou and X. Feng, *ACS Macro Lett.*, 2019, **8**, 1594-1598.
42. C. M. Byrne, S. D. Allen, E. B. Lobkovsky and G. W. Coates, *J. Am. Chem. Soc.*, 2004, **126**, 11404-11405.
43. L. Peña Carrodeguas, J. González-Fabra, F. Castro-Gómez, C. Bo and A. W. Kleij, *Chem. Eur. J.*, 2015, **21**, 6115-6122.
44. D. J. Darensbourg, W.-C. Chung, C. J. Arp, F.-T. Tsai and S. J. Kyran, *Macromolecules*, 2014, **47**, 7347-7353.
45. M. Winkler, C. Romain, M. A. R. Meier and C. K. Williams, *Green Chem.*, 2015, **17**, 300-306.
46. O. Hauenstein, M. Reiter, S. Agarwal, B. Rieger and A. Greiner, *Green Chem.*, 2016, **18**, 760-770.
47. D. J. Darensbourg, A. I. Moncada, W. Choi and J. H. Reibenspies, *J. Am. Chem. Soc.*, 2008, **130**, 6523-6533.
48. D. J. Darensbourg and A. I. Moncada, *Inorg. Chem.*, 2008, **47**, 10000-10008.
49. D. J. Darensbourg and A. I. Moncada, *Macromolecules*, 2009, **42**, 4063-4070.
50. D. J. Darensbourg and A. I. Moncada, *Macromolecules*, 2010, **43**, 5996-6003.
51. D. J. Darensbourg, A. I. Moncada and S.-H. Wei, *Macromolecules*, 2011, **44**, 2568-2576.
52. H.-L. Wu, J.-L. Yang, M. Luo, R.-Y. Wang, J.-T. Xu, B.-Y. Du, X.-H. Zhang and D. J. Darensbourg, *Macromolecules*, 2016, **49**, 8863-8868.
53. D. J. Darensbourg and S. J. Kyran, *ACS Catal.*, 2015, **5**, 5421-5430.
54. D. J. Darensbourg and S. J. Wilson, *Macromolecules*, 2013, **46**, 5929-5934.
55. M. Liu, B. Liu, L. Shi, F. Wang, L. Liang and J. Sun, *RSC Adv.*, 2015, **5**, 960-966.
56. N. Fanjul-Mosteirín, C. Jehanno, F. Ruipérez, H. Sardon and A. P. Dove, *ACS Sustain. Chem. Eng.*, 2019, **7**, 10633-10640.
57. J. Huang, C. Jehanno, J. C. Worch, F. Ruipérez, H. Sardon, A. P. Dove and O. Coulembier, *ACS Catal.*, 2020, **10**, 5399-5404.
58. E. M. López-Vidal, G. L. Gregory, G. Kociok-Köhn and A. Buchard, *Polym. Chem.*, 2018, **9**, 1577-1582.
59. A. P. Dove, *ACS Macro Lett.*, 2012, **1**, 1409-1412.
60. N. E. Kamber, W. Jeong, R. M. Waymouth, R. C. Pratt, B. G. G. Lohmeijer and J. L. Hedrick, *Chem. Rev.*, 2007, **107**, 5813-5840.
61. B. G. G. Lohmeijer, R. C. Pratt, F. Leibfarth, J. W. Logan, D. A. Long, A. P. Dove, F. Nederberg, J. Choi, C. Wade, R. M. Waymouth and J. L. Hedrick, *Macromolecules*, 2006, **39**, 8574-8583.
62. M. K. Kiesewetter, E. J. Shin, J. L. Hedrick and R. M. Waymouth, *Macromolecules*, 2010, **43**, 2093-2107.
63. Y. Shen, X. Chen and R. A. Gross, *Macromolecules*, 1999, **32**, 2799-2802.